BER Analysis in A Generalized UWB Frequency Selective Fading Channel With Randomly Arriving Clusters and Rays

Wei-Cheng Liu and Li-Chun Wang
Department of Communication Engineering
National Chiao Tung University, Hsinchu, Taiwan
lichun@cc.nctu.edu.tw, Tel: +886-3-5712121 ext 54511

Abstract— In this paper, we present an analytical method to evaluate the bit error rate (BER) of the ultra-wideband (UWB) system in the IEEE 802.15.4a standardized channel model. The IEEE 802.15.4a UWB channel model is more general and based on more measurements than the earlier IEEE 802.15.3a model. It also poses new challenge in analyzing UWB performance in such a channel. First, the power delay profile become a function of randomly arriving cluster and ray arrival time. Second, the signal amplitude in the IEEE 802.15.4a channel is modeled by a Nakagami random variable of which the Nakagami fading parameter is log-normally distributed. Thus, the signal amplitude is a nonlinear function of a log-normally distributed random variable. By means of counting integral of Lebesgue measure theory, the analytical expression for the BER performance in the IEEE 802.15.4a UWB channel is presented. We apply this analytical model to investigate the impacts of various UWB channel parameters on the system performance and provide some useful insights into the design of UWB transceiver.

Index Terms— Ultra-wideband (UWB), IEEE 802.15.4a channel model, bit error rate (BER).

I. Introduction

THE ultra-wideband (UWB) communications is a promising technique to achieve the objectives of higher data rates and better quality for the modern wireless systems. The complexity of the UWB channel has posed new challenges on performance analysis. Thus, for a more sophisticated channel model such as the IEEE 802.15.4a [1], the performance evaluation of UWB system is mainly performed by simulations.

Compared to traditional narrow-band channel, the UWB channel has two important properties. First, the bandwidth of the UWB signals is much wider than the coherence bandwidth of the channel. Thus, the severely frequency selective fading occurs in the frequency domain. Second, The large bandwidth of a UWB signal results in a arrival time with high resolution. Thus, the UWB waves arrive in many clusters and contain some non-Rayleigh multipath components.

A. Motivation and Challenges

Based on measurement results, the IEEE 802.15.4a has captured these important characteristics, but also pose new

challenges for performance analysis, which will be discussed next.

- Unlike the fixed number of impulse responses in a narrow-band channel, the UWB signals may arrive with random number of clusters and rays. In the IEEE 802.15.4a, the number of clusters is modeled as the Poisson random variable, and the inter-arrival time of the rays within a cluster is modeled by a hyperexponential random variable. Thus, computing the collected signal energy in a UWB channel with random number of both clusters and rays is complicated since one may need to find a joint distribution of *infinite* number of random variables.

- When the number of arrival rays in a very narrow time bin (or chip duration) is not large enough, the central limit theorem is no longer applicable to model the distribution of fading signal. Unlike a traditional Rayleigh random variable as in the narrow-band case, the multipath fading signal in the IEEE 802.15.4a UWB channel is characterized by a Nakagami m random variable of which the parameter m is a log-normal random variable related to the ray arrival time. Thus, the UWB signal amplitude become a multidimensional random variable and is a *nonlinear* function of another variable. The analysis of such a signal is rarely seen in the currently literature

Based on the IEEE 802.15.4a UWB channel model, a UWB signal is mathematically characterized by a joint continuous Nakagami m random variable for fading amplitude, a discrete Poisson random variable for cluster's number, and a discrete counting random variable with a hyperexponential distributed inter-arrival time. In [2], the author compared the IEEE 802.15.3a [3] and 802.15.4a channel model and concluded that the 4a model is more general and based on more measurements than the earlier 3a channel model. Thus, we are motivated to develop an analytical model to evaluate the impact of different UWB channel parameters on the system performance. There are nine sets of UWB channel parameters specified in the IEEE 802.15.4a for various environments. These channel parameters include the inter-cluster arrival rate, ray arrival rates (mixed Poisson model parameters), inter-cluster decay

constant, intra-cluster decay time constant parameters, the mean and variance of Nakagami m parameter, Nakagami m factor for the strongest components, and the alternative power delay profile (PDP) shape.

B. Related Work

Here we provide a literature survey on the related works in performance analysis of the UWB system. In [4], the authors derived the analytical BER formula for the binary and M-ary UWB systems with Walsh codes under the AWGN channel with multiple access interference (MAI). In [5], the authors studied the impacts of the interference from the universal mobile telecommunications system (UMTS)/wideband code division multiple access (WCDMA) system on the UWB systems. In [6], the BER formula of the UWB system under the flat and dispersive Rayleigh fading channels with timing jitters was derived. In [7], the authors analyzed the performance of a transmit-reference (TR) UWB system with an autocorrelation receiver under a slowly fading channel of which the amplitude is characterized by an appropriate moment generating function approach.

The BER formula in the IEEE 802.15.3a UWB channel model [3] was shown as a function of finite window size without considering the RAKE receiver in [8]. The statistics of the output signal-to-noise ratio (SNR) with the RAKE receiver under the IEEE 802.15.3a UWB channel were also obtained [9]. However, the explicit BER formula was unavailable and the shadowing effects are ignored. In [10], we derived the BER analytical formula with a coherent RAKE receiver in the *complete* IEEE 802.15.3a UWB channel model where shadowing is taken into account. In [11], an analytical expression for the SNR of the pulse position modulated (PPM) signal in a multi-input multi-output (MIMO) system was provided in a UWB channel characterized by Gamma distributed signal power with Poisson distributed arrival clusters and rays. In [12], the error performance of a zero-forcing (ZF) RAKE receiver in a MIMO system was analyzed in the frequency-selective UWB lognormal fading channels with a fixed number of clusters and rays.

C. Objective and Outline of This Paper

The objective of this paper is to evaluate BER performance with various UWB channel parameters specified in the IEEE 802.15.4a model. The rest of this paper is organized as follows. In Section II, we provide the required mathematical background about counting integrals to analyze the IEEE 802.15.4a channel. In Section III, we derive the analytical expression for the BER performance of the antipodal and orthogonal binary signals under the IEEE 802.15.4a UWB channel. We show the numerical results in Section IV and give our concluding remarks in Section V.

II. MATHEMATICAL BACKGROUND

The IEEE 802.15.4a channel model can be viewed as a random process. The random variables associated with the random process can be categorized into two kinds. First, the time

domain random variables, which contains the arrival time of all the clusters and rays, i.e., the variables $\{T_l\}$ and $\{\tau_{k,l}\}$, where the indices k and l can be any nonnegative integers. Second, the amplitude domain random variables, which contains the amplitudes of all the channel impulse, i.e., the variables $a_{k,l}$. Thus, in order to investigate the characteristics of the channel, we must consider infinite number of random variables. This makes the analysis very complicated.

Let us treat the problem in another way. Let us rewrite the channel impulse response $h(t)$ to (15) in [1] in a simpler form:

$$h(t) = \sum_k G_k \delta(t - T_k), \tag{1}$$

where T_k is the arrival time of the k-th multipath component, regardless it is a cluster or ray. We arrange $\{T_k\}$ such that it is a nondecreasing sequence. G_k is the gain of the k-th multipath component. In [14], the author focused on finding the characteristic function of the random variable Φ, which is the sum of path gains that arrive in the time window $[a, b]$. The mathematical expression of the random variable Φ can be written as

$$\Phi = \sum_k G_k I_{[a,b]}(T_k), \tag{2}$$

where

$$I_{[a,b]}(x) = \begin{cases} 1, & \text{if } x \in [a, b], \\ 0, & \text{if } x \notin [a, b]. \end{cases} \tag{3}$$

The purpose of defining $I_{[a,b]}(x)$ here is to consider the multipath components arriving within the time interval $[a, b]$.

The key idea to compute the statistics of Φ is the use of the counting integral [14]

$$\Phi = \sum_k \varphi(T_k, G_k) = \int_{-\infty}^{\infty} \int_0^{\infty} \varphi(s, g) N(ds \times dg), \tag{4}$$

where $N(\cdot)$ is the counting measure [15], $\varphi(s, g) = g I_{[a,b]}(s)$. The counting integral is the Lebesgue integral [16] defined based on the counting measure. That is, we first consider the value of the function φ within a small time interval ds and a small gain interval dg. Second, we integrate over all possible values of s and g, i.e., $s \in [0, \infty)$ and $g \in (-\infty, \infty)$. It is equivalent to sum up the value of the function $\varphi(T_k, G_k)$ for all k, which is the summation term in (4). By exploiting the counting integral, the original probability problem with infinitely many random variables has been transformed into a integral with only two dummy variables s and g. The remained problem is to find the characteristic function of Φ. The detail derivation can be found in [14].

III. BER ANALYSIS

A. Receiver Structure

Consider a coherent RAKE receiver with L_{RAKE} fingers. The received SNR γ_b is

$$\gamma_b = \frac{E_b}{N_0} \sum_{k=1}^{L} c_k^2 , \tag{5}$$

where E_b/N_0 is the bit SNR, c_k is the channel amplitude that appears at the k-th finger of the RAKE receiver. From [17] we know that the conditional error probability for binary signals for the coherent RAKE receiver is

$$P_2(\gamma_b) = Q\left(\sqrt{\gamma_b(1-\rho_r)}\right) \qquad (6)$$

where $\rho_r = -1$ for antipodal signals and $\rho_r = 0$ for orthogonal signals. Next we will derive the characteristic function of the received energy $\mathcal{E} \triangleq \sum_{k=1}^{L} c_k^2$ in the IEEE 802.15.4a UWB channel.

B. Characteristic Function of the Received Energy ($\mathcal{E}$)

In the following theorem, we give the formula of the characteristic function of $\mathcal{E}$. We modify and extend the result in [10] to the case of the IEEE 802.15.4a UWB channel.

Lemma 1: Let $\mathcal{L}_{T,t}(\nu)$ be the characteristic function of the squared gain of each path in the IEEE 802.15.4a UWB channel, where T and $t = T + \tau$ denotes the cluster arrival time and the ray arrival time, respectively. Also, let $e^{-\psi_\nu(T)}$ and $e^{-\Lambda J(\nu)}$ be the characteristic functions of a shot-noise random variables related to the ray arrival process with parameter λ and the cluster arrival process with parameter Λ, respectively. Then, it can be proved that the characteristic function of the received energy ($\mathcal{E}$) in the IEEE 802.15.4a UWB channel can be computed by

$$\Psi(\nu) = \mathcal{L}_{0,0}(\nu)e^{-\psi_\nu(0) - \Lambda J(\nu)}. \qquad (7)$$

Proof: In the IEEE 802.15.4a UWB channel, the ray arrival rate $\lambda(\tau)$ is a function of τ. Thus, different from the 3a case, we have to redefine the function $\psi_\nu(T)$ by putting $\lambda(\tau)$ into the integral:

$$\psi_\nu(T) = \begin{cases} \int_{\max(a,T)}^{b}[1 - \mathcal{L}_{T,t}(\nu)]\lambda(t-T)dt, & T \le b, \\ 0, & T > b, \end{cases} \qquad (8)$$

The term $\lambda(\tau)$ can be found in Theorem 2. ∎

Theorem 1: Consider a RAKE receiver with L_{RAKE} fingers in the IEEE 802.15.4a UWB channel. The characteristic function $\mathcal{L}_{T,t}(\nu)$ can be computed by

$$\mathcal{L}_{T,t}(\nu) = (1 - j\nu\Omega/m)^{-m} \qquad (9)$$

where

$$\Omega = \frac{1}{\gamma_l}\exp\left(-\frac{T}{\Gamma} - \frac{t-T}{\gamma_l}\right) \qquad (10)$$

and

$$m = \exp\left(m_0 + \widehat{m}_0^2/2\right). \qquad (11)$$

The parameter γ_l is defined in (20) in [1].

Proof: See Appendix I. ∎

Theorem 2: The parameter λ in Lemma 1 is a function of τ and can be expressed as

$$\lambda(\tau) = \begin{cases} \frac{\beta\lambda_1 e^{-\lambda_1\tau} + (1-\beta)\lambda_2 e^{-\lambda_2\tau}}{\beta e^{-\lambda_1\tau} + (1-\beta)e^{-\lambda_2\tau}}, & \tau \ge 0, \\ 0, & \tau < 0. \end{cases} \qquad (12)$$

Proof: See Appendix II. ∎

The equations for calculating $\psi_\nu(T)$ and $J(\nu)$ can be found in Theorem 2 in [10].

With characteristic function of $\mathcal{E}$, i.e. $\Psi(\nu)$ in (7), the probability density function (PDF) of $\mathcal{E}$ can be computed by the Gauss-Hermite formula as follows:

$$\begin{aligned}
f_\mathcal{E}(x) &= \frac{1}{2\pi}\int_{-\infty}^{\infty}\Psi(\nu)e^{-jx\nu}d\nu \\
&\approx \frac{1}{2\pi}\sum_{k=1}^{N^{(H)}}w_k^{(H)}\Psi(\nu)e^{-jx\nu}e^{\nu^2}\Big|_{\nu=x_k^{(H)}}.
\end{aligned} \qquad (13)$$

Combining (9), (13), and (16) and (17) in [10], the BER of the RAKE receiver in the IEEE 802.15.4a UWB channel can be computed as

$$\begin{aligned}
P_2 &= \mathbb{E}_\mathcal{E}\left[Q\left(\sqrt{(1-\rho_r)\frac{E_b}{N_0}\mathcal{E}}\right)\right] \\
&= \int_0^\infty Q\left(\sqrt{(1-\rho_r)\frac{E_b}{N_0}x}\right)f_\mathcal{E}(x)dx \\
&= \frac{1}{2\pi}\left(1 - j\frac{\nu}{\gamma_0\exp\left(m_0 + \widehat{m}_0^2/2\right)}\right)^{-\exp\left(m_0 + \widehat{m}_0^2/2\right)} \\
&\quad \sum_{k=1}^{N^{(H)}}w_k^{(H)}\exp\left(-\frac{1}{2}\lambda(L-1)T_c\sum_{p=1}^{N^{(L)}}w_p^{(L)} \right. \\
&\quad [1 - \mathcal{L}_{0,t}(\nu)]|_{t=\frac{1}{2}(L-1)T_c(x_P^{(L)}+1)}\Big) \\
&\quad \exp\left(-\frac{1}{2}\Lambda(L-1)T_c\sum_{i=1}^{N^{(L)}}w_i^{(L)}\right. \\
&\quad \left.\left[1 - \mathcal{L}_{T,T}(\nu)e^{-\lambda\psi_\nu(T)}\right]\Big|_{T=\frac{1}{2}(L-1)T_c(x_i^{(L)}+1)}\right) \\
&\quad \int_0^\infty Q\left(\sqrt{(1-\rho_r)\frac{E_b}{N_0}x}\right)\exp(-jx\nu)dx \\
&\quad \exp(\nu^2)\big|_{\nu=x_k^{(H)}}.
\end{aligned} \qquad (14)$$

C. Discussion

It is possible to apply the above analytical method to the generalized UWB frequency selective fading channel with any given fading distribution, PDP, and the distribution of cluster and ray inter-arrival time. For a give PDP, we only need to express it as a function of T and t and place it in (10) as the procedure in Appendix I. For a given PDF of the fading amplitude, we can first find the PDF of the squared amplitude as in (17) and use (18) to find $\mathcal{L}_{T,t}(\nu)$. For any given PDF of ray inter-arrival time, we can use the same method as in Appendix II to find the intensity function and $\lambda(\tau)$ and applied it in (7). For any given PDF of cluster inter-arrival time, we can also find its intensity function $\Lambda(T)$. Since it is a function of T we need to redefine the function $J(\nu)$ as

$$J(\nu) = \int_0^b \Lambda(T)[1 - \mathcal{L}_{T,T}(\nu)e^{-\psi_\nu(T)}]dT . \qquad (15)$$

That is, we put the function $\Lambda(T)$ into the integrand and integrate it with respect to T. On the other hand, the function

$\Psi(\nu)$ should be rewritten as

$$\Psi(\nu) = \mathcal{L}_{0,0}(\nu)e^{-\psi_\nu(0)-J(\nu)} \quad . \tag{16}$$

IV. NUMERICAL RESULTS

We will apply the developed analytical model to evaluate the effect of different UWB channel parameters on the BER performance of the system, including cluster arrival rate Λ, inter-cluster decay constant Γ, intra-cluster decay constant γ_0, and ray arrival parameters (λ_1, λ_2, and β). In our recently work [13], we have validated the correctness of the analytical model by simulations in a simple case. In the following, we consider a RAKE receiver with 10 fingers and the CM1 model in the IEEE 802.15.4a standard.

A. Impact of the Inter-Cluster Arrival Rate Λ on BER

Figure 1 shows the BER v.s. E_b/N_0 for various inter-cluster arrival rate $\Lambda = 0.01, 0.1, 0.5$, and 1. We can see that when the cluster arrival rate increases, the BER decreases. This is because when the inter-cluster arrival rate increases, more clusters arrive in the time interval $[0, (L-1)T_c]$ and the RAKE receiver can collect more energy of the channel impulse, thereby improving the BER.

B. Impact of the Inter-Cluster Decay Constant Γ on BER

Figure 5 shows the BER v.s. E_b/N_0 for CM1 by analysis. The number of the RAKE receiver fingers is 10. We show four curves with the inter-cluster decay constant $\Gamma = 0.1, 1, 10$, and 100. We can see that when Γ increases, the BER decreases. This is because according to (21) in [1], when Γ increases, the Ω_l, which is the integrated energy of the lth cluster, will increases, and the RAKE receiver can collect more energy of the channel impulse, thus the BER will decrease.

C. Impact of the Ray Arrival Parameter λ_1 on BER

Figure 2 shows the BER v.s. E_b/N_0 for different value of ray-arrival parameter $\lambda_1 = 0.01, 0.1, 1$, and 10. One can see that when λ_1 increases, the BER decreases. This is because when λ_1 increases, more rays in each cluster arrive in the time interval $[0, (L-1)T_c]$ and the RAKE receiver can collect more energy of the channel impulse. Compared with the impact of the cluster arrival rate, changing λ_1 leads to less variation on the BER than the cluster arrival rate does. It is reasonable because the cluster arrival rate is a macroscopic parameter that influences every clusters and λ_1 is a microscopic parameter that influences only rays within each cluster.

D. Impact of the Ray Arrival Parameter λ_2 on BER

Figure 3 shows the BER v.s. E_b/N_0 parameter $\lambda_2 = 0.01, 0.1, 1$, and 10. When λ_2 increases, the BER decreases.

This is because when λ_2 increases, more rays in each cluster arrive in the time interval $[0, (L-1)T_c]$ and the RAKE receiver can collect more energy of the channel impulse. Thus the BER with larger λ_2 will improve BER performance. Furthermore, Compared with Figure 2, changing λ_2 influences the BER more significantly than λ_1 the BER. It is reasonable because for the CM1 in IEEE 802.15.4a standard, $\beta = 0.095$.

According to (18) in [1], we can see that ray interarrival time has the probability 0.095 decided by the parameter λ_1 and has the probability of 0.905 decided by the parameter λ_2. Thus λ_2 has more significant impact on BER than λ_1 does.

E. Impact of the Ray Arrival Parameter β on BER

Figure 4 shows the BER v.s. E_b/N_0 for different values of $\beta = 0, 1/3, 2/3$, and 1. As β increases, the BER decreases. According to (18) in [1], when β increases, the ray process has the higher probability to choose the arrival rate λ_1 rather than λ_2. For CM1, $\lambda_1 = 1.54$ and $\lambda_2 = 0.15$. From the discussion in the last two subsection, we know that the higher the ray arrival rate is, the lower the BER. This phenomenon is similar to the cluster. As the cluster arrival rate increases, the BER decreases, as we have seen in Subsection IV-A.

F. Impact of the Intra-Cluster Decay Constant γ_0 on BER

Figure 6 shows the BER v.s. the intra-cluster decay constant γ_0 for $E_b/N_0 = 5, 10$, and 15 dB. When γ_0 increases, the BER first increases and then decreases. This phenomenon can be explained as follows. Based on (20) in [1], a larger value of γ_0 also leads to a larger value of γ_l. According to (19) in [1], for a small value of γ_l, the term $1/\gamma_l$ dominates the BER performance, which cause the decrease of Ω_l and the increase of BER. When γ_l is large, the exponential term dominates and therefore Ω_l increases and BER decreases. The maximum of the BER occurs at $\gamma_0 = 30, 40$, and 100 for $E_b/N_0 = 5, 10$, and 15 dB, respectively.

V. CONCLUSIONS

In this paper, we have derived the BER analytical formula for a coherent RAKE receiver under the IEEE 802.15.4a UWB channel model. Our proposed analytical BER formula can obtain the BER values quickly, compared to the computer simulation. Further, we also discuss the impact of various parameters of the IEEE 802.15.4a UWB channel model on BER. Furthermore, it is worthwhile to emphasize that the suggested analytical method can be applied to other multipath channel models with any given fading distribution, PDP, and cluster and ray inter-arrival time distributions.

APPENDIX I
PROOF OF THEOREM 1

From (24) in [1], we can easily find the PDF of $x = a^2$ by exploiting the resulting of Example 7b in [18]. That is,

$$
\begin{aligned}
f_x(x) &= \frac{1}{2\sqrt{x}}\left[f_a(\sqrt{x}) + f_a(-\sqrt{x})\right] \\
&= \begin{cases} \frac{\exp\left(-\frac{mx}{\Omega}\right)\left(\frac{mx}{\Omega}\right)^m}{x\Gamma(m)}, & x \geq 0, \\ 0, & x < 0. \end{cases}
\end{aligned} \tag{17}
$$

The characteristic function of x is

$$
\begin{aligned}
\mathcal{L}_{T,t}(\nu) &= \int_{-\infty}^{\infty} f_x(x) e^{j\nu x} dx \\
&= (1 - j\nu\Omega/m)^{-m}.
\end{aligned} \tag{18}
$$

The term $\Omega = E\{x\}$ is defined in (19) in [1]. To fit it into our formula, we substitute T_l by T and $M_{cluster}$ by its mean, zero, in (21) in [1] and $\tau_{k,l}$ by $(t - T)$ in (19) in [1]. Then we can get (10).

Finally, we set m to its mean and get (11). The mean is given by (4) in [19].

APPENDIX II
PROOF OF THEOREM 2

According to (18) in [1], the PDF of interarrival time of ray is

$$
f(\tau) = \begin{cases} \beta\lambda_1 e^{-\lambda_1 \tau} + (1-\beta)\lambda_2 e^{-\lambda_2 \tau}, & \tau \geq 0, \\ 0, & \tau < 0. \end{cases} \tag{19}
$$

The cumulative distribution function (CDF) is

$$
\begin{aligned}
F(\tau) &= \int_{-\infty}^{\tau} f(x) dx \\
&= \begin{cases} 1 - \beta e^{-\lambda_1 \tau} - (1-\beta)e^{-\lambda_2 \tau}, & \tau \geq 0, \\ 0, & \tau < 0. \end{cases}
\end{aligned} \tag{20}
$$

The parameter λ in Lemma 1 is the intensity function [20] of the interarrival time of rays:

$$
\begin{aligned}
\lambda(\tau) &= \frac{f(\tau)}{1 - F(\tau)} \\
&= \begin{cases} \frac{\beta\lambda_1 e^{-\lambda_1 \tau} + (1-\beta)\lambda_2 e^{-\lambda_2 \tau}}{\beta e^{-\lambda_1 \tau} + (1-\beta)e^{-\lambda_2 \tau}}, & \tau \geq 0, \\ 0, & \tau < 0. \end{cases}
\end{aligned} \tag{21}
$$

The ray arrival rate is a function of time τ, which means the ray arrival is a nonhomogeneous Poisson process. Note that when $\beta = 1$, the PDF in (19) reduces to the exponential PDF and the intensity function reduces to the constant λ_1. This case corresponds to a homogenous Poisson process.

REFERENCES

[1] A. F. Molisch et al., "IEEE 802.15.4a channel model - final report," IEEE 802.15 WPAN Low Rate Alternative PHY Task Group 4a (TG4a), Tech. Rep., Nov. 2004.

[2] A. F. Molisch, "Ultrawideband propagation channels-theory, meausrement, and modeling," *IEEE Trans. on Veh. Technol.*, vol. 54, no. 5, pp. 1528–1545, Sept. 2005.

[3] J. Foerster, et. al., "Channel modeling sub-committee report final," *IEEE P802.15 Wireless Personal Area Networks, P802.15-02/490r1-SG3a*, Feb. 2003.

[4] K. Eshima, Y. Hase, S. Oomori, F. Takahashi, and R. Kohno, "M-ary UWB system using Walsh codes," *IEEE Conference on Ultra Wideband Systems and Technologies*, pp. 37–40, May 21–23, 2002.

[5] M. Hämäläinen, R. Tesi, and J. Iinatti, "On the UWB system performance studies in AWGN channel with interference in UMTS band," *IEEE Conference on Ultra Wideband Systems and Technologies*, pp. 321–325, May 21–23, 2002.

[6] İ. Güvenç and H. Arslan, "Performance evaluation of UWB systems in the presence of timing jitter," *IEEE Conference on Ultra Wideband Systems and Technologies*, pp. 136–141, Nov. 16–19, 2003.

[7] T. Q. S. Quek and M. Z. Win, "Ultrawide bandwidth transmitted-reference signaling," *IEEE International Conference on Communications*, vol. 6, pp. 3409–3413, June 20–24, 2004.

[8] J. A. Gubner and K. Hao, "A computable formula for the average bit-error probability as a function of window size for the IEEE 802.15.3a UWB channel model," *IEEE Trans. Microwave Theory Tech.*, vol. 54, no. 4, pp. 1762–1777, Apr. 2006.

[9] K. Hao and J. A. Gubner, "Performance measures and statistical quantities of RAKE receivers using maximal-ratio combining on the IEEE 802.15.3a UWB channel model," *IEEE Trans. on Wireless Commun.*, submitted for publication. [Online]. Available: http://homepages.cae.wisc.edu/~gubner/HaoGubnerTWaf2col.pdf

[10] W.-C. Liu and L.-C. Wang, "Performance analysis of pulse based ultra-wideband systems in the highly frequency selective fading channel with cluster property," *IEEE Vehicular Technology Conference*, vol. 3, pp. 1459–1463, May 7–10, 2006.

[11] L.-C. Wang, W.-C. Liu, and K.-J. Shieh, "On the performance of using multiple transmit and receive antennas in pulse-based ultrawideband systems," *IEEE Trans. on Wireless Commun.*, vol. 4, no. 6, pp. 2738–2750, Nov. 2005.

[12] H. Liu, R. C. Qiu, and Z. Tian, "Error performance of pulse-based ultra-wideband MIMO systems over indoor wireless channels," *IEEE Trans. on Wireless Commun.*, vol. 4, no. 6, pp. 2939–2944, Nov. 2005.

[13] W.-C. Liu and L.-C. Wang, "BER analysis of the IEEE 802.15.4a channel model with RAKE receiver," to appear in *IEEE Vehicular Technology Conference*, Sep. 2006.

[14] K. Hao and J. A. Gubner, "The distribution of sums of path gains in the IEEE 802.15.3a UWB channel model," *IEEE Trans. on Wireless Commun.*, to appear. [Online]. Available: http://eceserv0.ece.wisc.edu/~gubner/HaoGubnerTWdistFinal.pdf

[15] Mathwizard and Drummond, "Counting measure," *PlanetMath*. [Online]. Available: http://planetmath.org/encyclopedia/CountingMeasure.html

[16] E. M. Stein and R. Shakarchi, *Real Analysis : Measure Theory, Integration, and Hilbert Spaces*. Princeton University Press, 2005.

[17] J. G. Proakis, *Digital Communications*, 4th ed. Boston: McGraw-Hill, 2001.

[18] S. Ross, *A First Course in Probability*, 5th ed. Prentice-Hall International, Inc., 1998.

[19] E. W. Weisstein, "Log-normal distribution," *MathWorld–A Wolfram Web Resource*. [Online]. Available: http://mathworld.wolfram.com/LogNormalDistribution.html

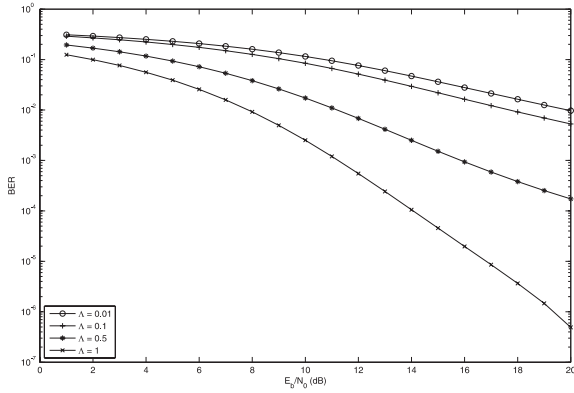[20] A. Andersson, "The intensity concept," *SICS Technical Report ISRN:SICS-T-2000/03-SE T2000:03 ISSN 1100-3154*. [Online]. Available: http://www.sics.se/~aeg/report/node11.html

Fig. 1. The BER v.s. E_b/N_0 for the RAKE receiver with 10 fingers in the IEEE 802.15.4a UWB channel CM1. The inter-cluster arrival rate Λ is 0.01, 0.1, 0.5, and 1.
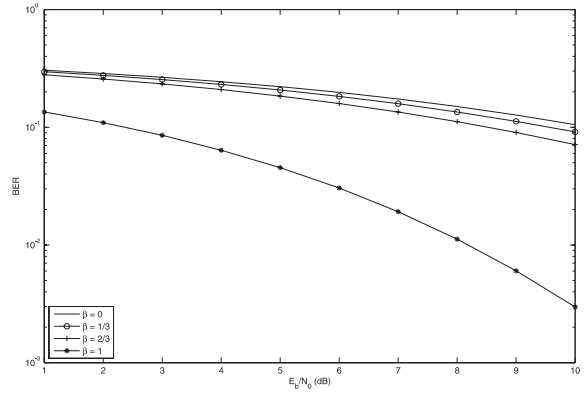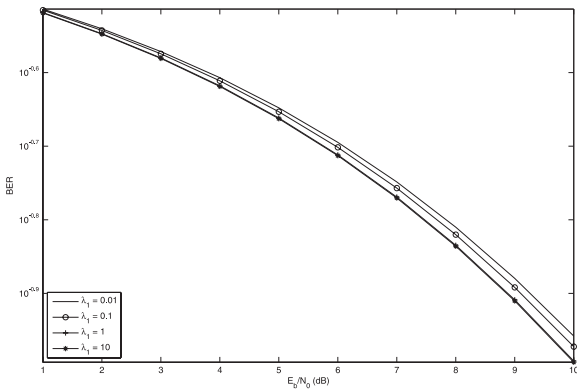

Fig. 2. The BER v.s. E_b/N_0 for the RAKE receiver with 10 fingers in the IEEE 802.15.4a UWB channel CM1. The parameter λ_1 is 0.01, 0.1, 1, and 10.

Fig. 3. The BER v.s. E_b/N_0 for the RAKE receiver with 10 fingers in the IEEE 802.15.4a UWB channel CM1. The parameter λ_2 is 0.01, 0.1, 1, and 10.

Fig. 4. The BER v.s. E_b/N_0 for the RAKE receiver with 10 fingers in the IEEE 802.15.4a UWB channel CM1. The parameter β is 0, 1/3, 2/3, and 1.
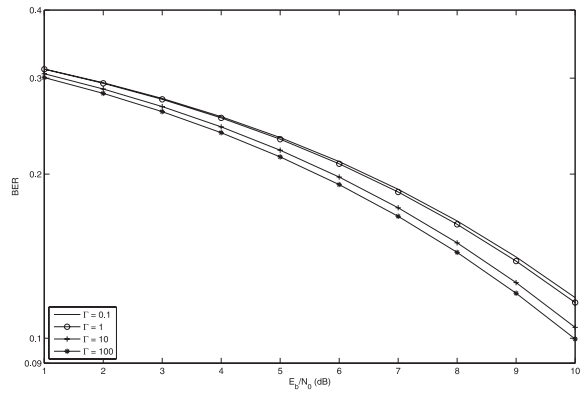

Fig. 5. The BER v.s. E_b/N_0 for the RAKE receiver with 10 fingers in the IEEE 802.15.4a UWB channel CM1. The inter-cluster decay constant Γ is 0.1, 1, 10, and 100.
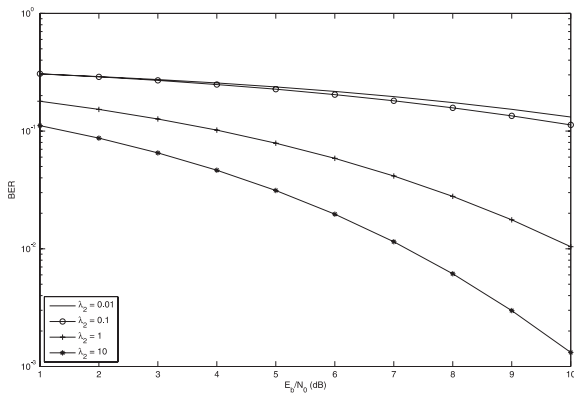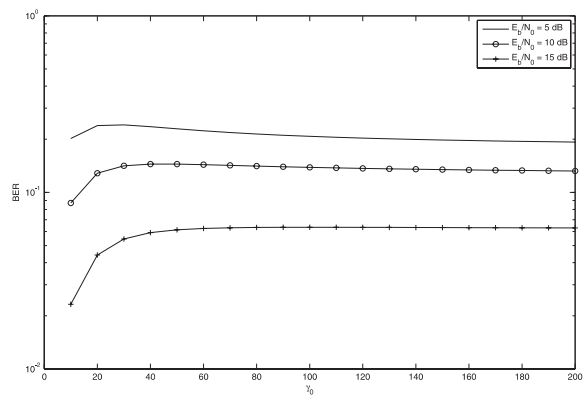

Fig. 6. The BER v.s. γ_0 for the RAKE receiver with 10 fingers in the IEEE 802.15.4a UWB channel CM1. E_b/N_0 is 5 dB, 10 dB, and 15 dB.